FEBS Letters 581 (2007) 2527–2533

Identification and characterization of DUSP27, a novel dual-specific protein phosphatase

Ilan Friedberg, Konstantina Nika, Lutz Tautz, Kan Saito, Fabio Cerignoli, Iddo Friedberg, Adam Godzik, Tomas Mustelin*

The Burnham Institute for Medical Research, North Torrey Pines Road, La Jolla, CA 92037, USA

Received 17 March 2007; revised 8 April 2007; accepted 18 April 2007

Available online 30 April 2007

Edited by Berend Wieringa

Abstract A novel human dual-specific protein phosphatase (DSP), designated DUSP27, is here described. The *DUSP27* gene contains three exons, rather than the predicted 4–14 exons, and encodes a 220 amino acid protein. DUSP27 is structurally similar to other small DSPs, like VHR and DUSP13. The location of *DUSP27* on chromosome 10q22, 50 kb upstream of *DUSP13*, suggests that these two genes arose by gene duplication. DUSP27 is an active enzyme, and its kinetic parameters and were determined. DUSP27 is a cytosolic enzyme, expressed in skeletal muscle, liver and adipose tissue, suggesting its possible role in energy metabolism.

Keywords: Dual-specific protein phosphatase; Protein tyrosine phosphatase; DUSP27; DUPD1; Enzyme modeling; Enzyme localization

1. Introduction

Reversible protein tyrosine phosphorylation, mediated by protein tyrosine kinases (PTKs) and protein tyrosine phosphatases (PTPs), plays a vital role in the regulation of multiple processes within the living cell and in its interactions with extracellular factors [1]. While many PTKs have been extensively studied, much less attention has been paid to their counterparts, the PTPs. New and unexpected PTP functions are still discovered, including mitochondrial tasks, which affect insulin secretion [2] and apoptosis [3], as well as control of vesicle fusion [4], and regulation of potassium channels [5].

More than a hundred genes for PTPs are present in the human genome and about 60 of them are structurally classified as dual-specific phosphatases (DSPs). Among these was a single gene, which was not covered by any expressed signal tags [1]. This computationally predicted ORF (gi:4265934, XM_291741.4), designated *DUPD1* (for *du*al specific phosphatase and *p*ro isomerase *d*omain containing 1), had 446 amino acid residues and contained a cyclophilin-like domain in addition to its catalytic phosphatase domain. The pro-isomerase domain, however, was later removed from the predicted *DUPD1* sequence, leaving the name *DUPD1* a misnomer. The gene is now officially referred to as dual specificity phosphatase 27 *(DUSP27)*.

In this study we set out to find whether this predicted enzyme is expressed, and, if so, to determine its structure and to begin its characterization.

2. Materials and methods

2.1. Materials

Human cDNA was obtained from BD Biosciences-Clontech (Palo Alto, CA) and from Biochain (Hayward, CA). Primers were obtained from Invitrogen Corporation (Carlsbad, CA), and from Valuegene (San Diego, CA). Titanium Taq DNA polymerase kit and Platinum Taq DNA polymerase were obtained from BD Biosciences-Clontech and from Invitrogen Corporation, respectively. Membranes for Northern blot were obtained from Ambion (Austin, TX) and from Biochain. [^{32}P]dCTP was purchased from Amersham (Piscataway, NJ). QIAquick Gel Extraction Kit, QIAquick PCR purification kit, and Ni-NTA-Agarose beads were from QIAGEN (Valencia, CA). Primer Kit II, the plasmid pET28a(+) and *E. coli* BL21 (DE3) cells were from Stratagene (La Jolla, CA); the plasmid pEF3HA was designed in our laboratory [6]. Phosphotyrosine and phosphothreonine were obtained from Sigma–Aldrich (St. Louis, MO) and phosphoserine from PM Biochemicals (Solon, OH). Biomol Green was purchased from Biomol (Plymouth Meeting, PA), and 6,8-difluoro-4-methylumbelliferyl phosphate (DiFMUP) was obtained from Invitrogen Corporation.

2.2. PCR amplification and DNA sequencing

DUSP27 was sought for in human cDNA libraries by employing PCR, using Titanium Taq polymerase kit with the primers ATG ACA TCT GGA GAG TGA AGA CAA GC and CTA CAC TCC CTG CCA TCC TC, matching nucleotides 1–27 and 741–721, respectively, of the published DNA sequence of *DUSP27* (741 nucleotides in 4 exons). Detection of 5′ non-coding and 3′ non-translated regions of *DUSP27* was performed by using PCR and sequencing, with the primers AAC CAG CTG CAG AAA GGA GA and AAT GTA GAG CTT GGG CCA GA, corresponding to nucleotides 40–20 before the initiation codon, and nucleotides 100–120 after the stop codon, respectively. PCR was carried out by using either Titanium Taq DNA polymerase kit or Platinum Taq DNA polymerase, according to the manufacturer instructions, for 35 cycles. The PCR products were purified by using either QIIAquick PCR purification kit, or by Agarose gel electrophoresis, followed by DNA extraction with QIAquick Gel Extraction Kit. The DNA preparations were sequenced in the Burnham Institute facilities.

2.3. Northern blots

DUSP27 DNA was isolated from pET28a(+) plasmid containing the *DUSP27* insert, using the enzyme EcoRI, and purified by gel electro-

*Corresponding author. Fax: +1 858 713 9925.
E-mail address: tmustelin@burnham.org (T. Mustelin).

Abbreviations: DiFMUP, 6,8-difluoro-4-methylumbelliferyl phosphate; DSP, dual-specific protein phosphatase; DUPD1, dual-specific protein phosphatase domain containing 1; DUSP27, dual-specific phosphatase 27; His_6-DUSP, histidine epitope-tagged DUSP27; HA-DUSP27, hemagglutinin epitope-tagged DUSP27; InsP, inositol-phosphate; pNPP, *p*-nitrophenyl phosphate; PTK, protein tyrosine kinase; PTP, protein tyrosine phosphatase; VHR, VH1 related

0014-5793/$32.00
doi:10.1016/j.febslet.2007.04.059

phoresis and the QIAquick Gel Extraction Kit. The isolated *DUSP27* DNA was radioactively labeled with [^{32}P]-dCTP, using Primer Kit II, according to the manufacturer instructions, and was used as a probe for Northern blot. Charged nylon membranes, containing RNA samples from various tissues, were incubated with the radioactive probe, washed and exposed to X-ray film.

2.4. Three-dimensional model

The DUSP27 model was built using a comparative modeling approach, based on the structure of VHR (PDB code 1vhr) and by using fold prediction metaserver alignment [7]. Modeling was done by SWISS-MODEL [8]. Images were generated using iMol version 0.30 (Pirx) and MOLCAD as implemented in SYBYL version 7.0 (Tripos).

2.5. Expression plasmids, recombinant protein, and antibodies

The cDNA for *DUSP27* was cloned into the prokaryotic expression vector pET28a(+), and into eukaryotic plasmid pEF3HA, which add N-terminal His_6 tag, or C-terminal hemagglutinin tag (HA-tag) to the insert, respectively. Recombinant DUSP27 protein was produced in *E. coli* BL21 (DE3) cells, transformed with pET28a(+) plasmid containing the DUSP27 insert. The His_6-DUSP27 was isolated from the

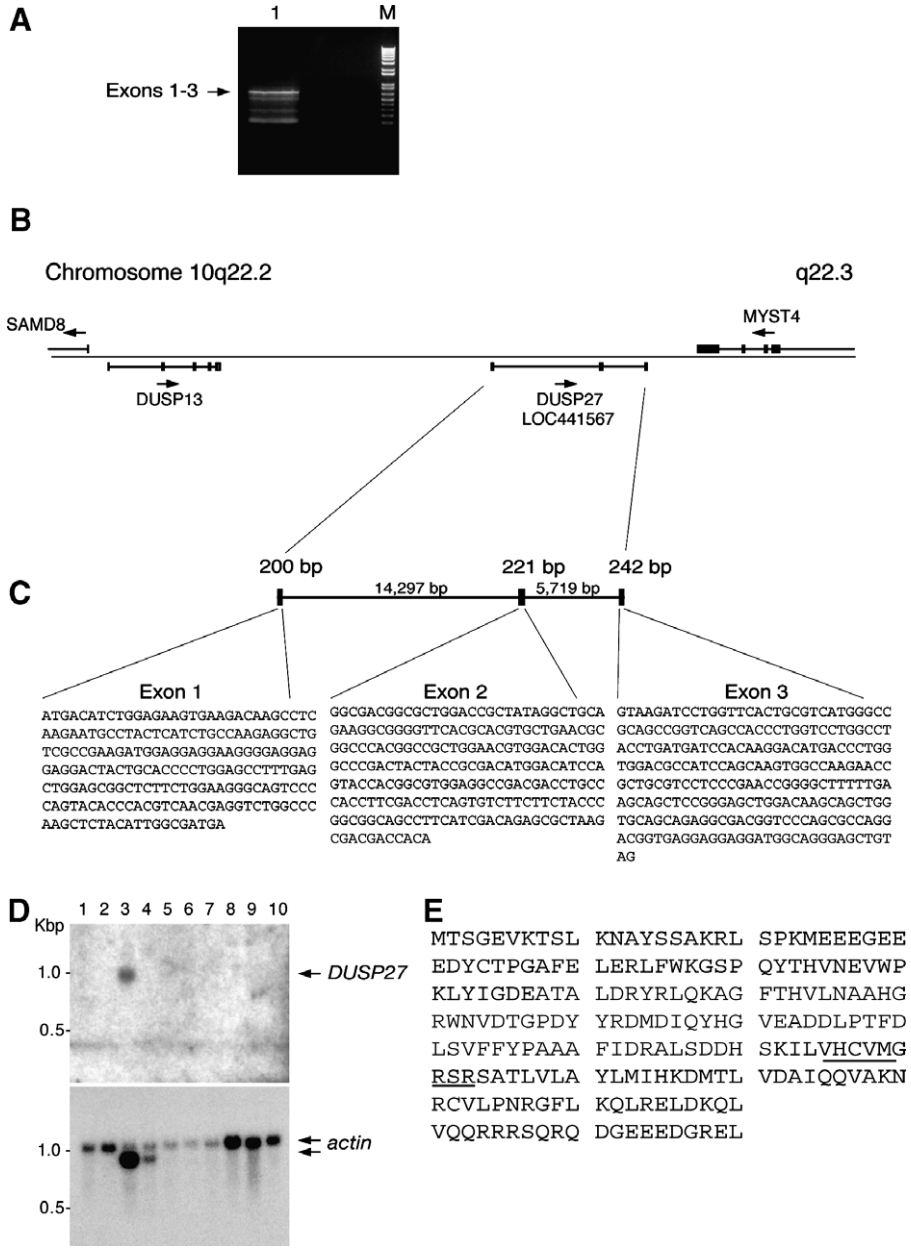

Fig. 1. Organization of the *DUSP27* gene and its amino acid sequence. (A) Polymerase chain reaction amplification of skeletal muscle cDNA resulted in a DNA (lane 1), the sequence of which composed of the protein expression parts of exons 1, 2, and 3. M, MW markers. (B) Region q22.2–q22.3 of human chromosome 10, including *DUSP27* gene (LOC441567). Note that *DUSP13* is ~50 kb upstream of *DUSP27*. (C) Exon and intron structure of the *DUSP27* gene. The untranslated sequences of exon 1 and 3 are not shown. (D) Northern blot, using radioactively labeled *DUSP27* DNA as a probe, and a membrane containing RNA from (1) brain, (2) placenta, (3) skeletal muscle, (4) heart, (5), kidney (6), pancreas, (7) liver, (8), lung, (9) spleen, and (10) colon. (E) Deduced amino acid sequence of *DUSP27*. The protein sequences related to exons 1 and 3 are in black, while the sequence related to exon 2 is in gray. Amino acids of the active site of the enzyme are underlined.

E. coli lysate by using Ni-NTA-agarose beads column. Polyclonal rabbit antisera were raised against this recombinant protein and were used at 1:1000 dilution.

2.6. Phosphatase activity assay

The reaction mixture (0.1 ml) for kinetics parameters determination contained 0.1 M Bis–Tris buffer, pH 6.0, 0.15 M NaCl, 1 mM dithiotreitol, 0.125 to 8.0 mM *p*-nitrophenyl phosphate (pNPP), and 1.2 μg of His_6-DUSP27. After 20 min incubation at 30 °C the reaction was terminated by addition of 0.1 ml of 0.1 M NaOH, and the absorbance at 405 nm was read by using Elx808 microplate reader (Bio-Tek Instruments). The K_m and K_{cat} values were determined by fitting the data in to the Michaelis–Menten equations, using non-linear regression and the program GraphPad Prism® (version 4.0). The substrate specificity of DUSP27 was determined under similar conditions, except for using 10 mM phospho-amino acids as substrates. The reaction was terminated after 45 min incubation by addition of 0.2 ml Biomol Green, and the absorbance was read at 620 nm. The pH dependence activity was determined under similar conditions, except for using 15 ng DUSP27, 20 μM DiFMUP as a substrate, and the following buffers: sodium citrate for pH 4.5/5.0/5.5, Bis–Tris for pH 6.0/6.5/7.0, and Tris·HCl for pH 7.5/8.0/8.5. Product fluorescence was determined at 460 nm (excitation at 340 nm) 10 min after reaction initiation.

2.7. Mouse tissues and cell lines

Mouse tissues were dissected from Balb/c mice. HeLa and Jurkat cells were grown in RPMI 1640 medium supplemented with 10% bovine calf serum, 2 mM L-glutamine, 1 mM sodium pyruvate, non-essential amino acids, 100 U/ml penicillin G and 100 μg/ml streptomycin. HeLa cells were transfected with 5–10 μg DNA by lipofection and Jurkat cells by electroporation. Empty vector was added to control samples.

2.8. SDS–PAGE and immunoblotting

Cell lysis buffer contained 20 mM Tris·HCl, pH 7.5, 150 mM NaCl 5 mM EDTA, 1% Nonidet P-40, 1 mM Na_3VO_4, 10 μg/ml aprotinin, 10 μg/ml leupeptin, 100 μg/ml soybean trypsin inhibitor and 1 mM phenylmethylsulphonyl fluoride. Cell lysates were clarified by centrifugation at $16000 \times g$ for 20 min. Then samples were subjected to

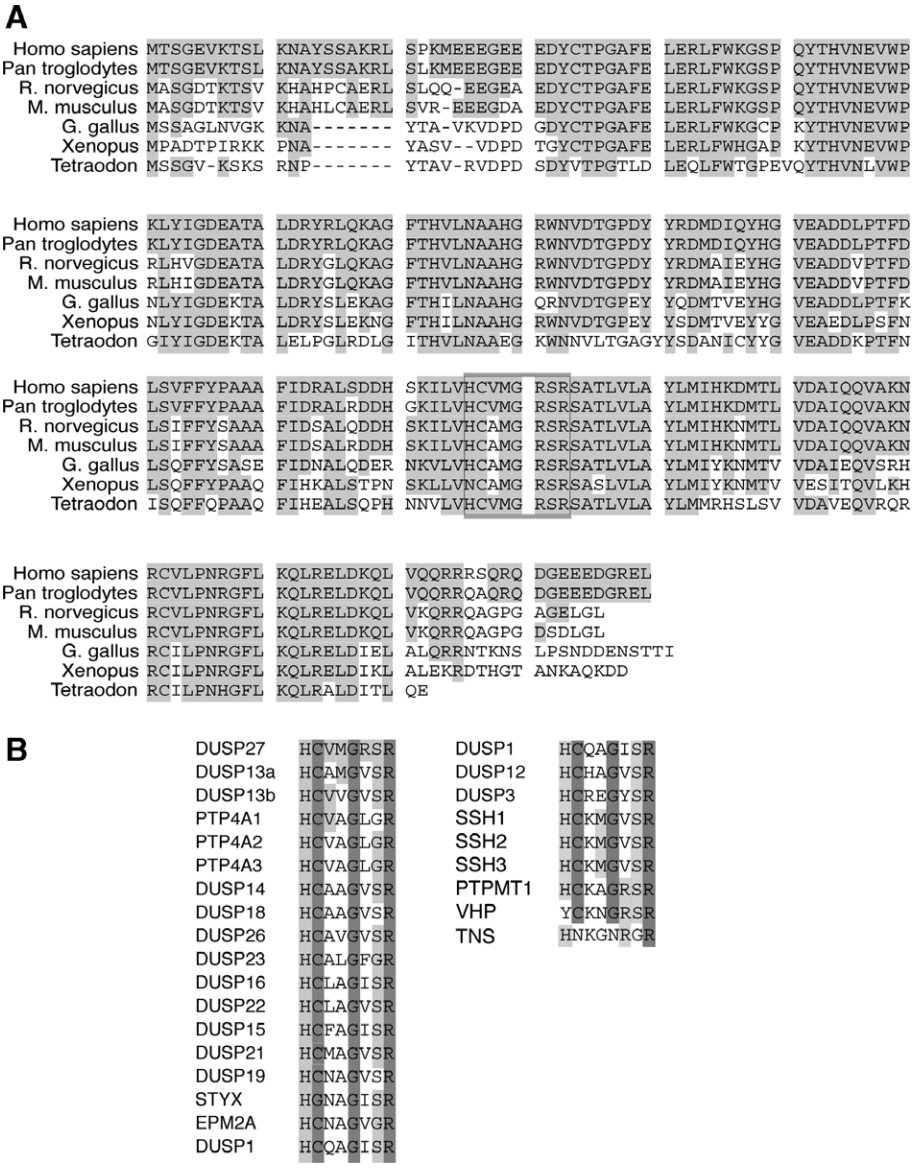

Fig. 2. Species orthologs and human homologs of DUSP27. (A) Alignment of human, chimpanzee, rat, mouse, chicken, frog, and fish *DUSP27*. Gray shading indicates identity to human DUSP27. The PTP signature sequence is boxed. (B) PTP signature sequence in DUSP27 compared the closest human homologs.

SDS–PAGE, electrophoretically transferred to nitrocellulose filters, which were immunoblotted with 1:1000 anti-DUSP27, followed by anti-rabbit-Ig-peroxidase, and the blots were developed by using ECL kit (Amersham).

3. Results and discussion

3.1. 'Cyclophilin-like' is not cyclophilin-like

During our efforts to catalogue all functional PTP genes in the human genome, we came across a computationally predicted ORF encoding 446 amino acid residues and two catalytic domains, a proline isomerase and a DSP [1]. To determine whether this is a functional gene we used a combination of primers for the conserved sequence in the enzyme. The largest obtained amplification product (Fig. 1A) consisted of a sequence that represented only three of the predicted protein-coding sequences, 200, 221, and 242 bp, respectively (Fig. 1B and C). Thus, the computationally predicted four to fourteen exons in various databases likely include intronic sequences erroneously designated as exons. The conclusion that the protein-coding part of the mRNA consists of 663 bp was sup-

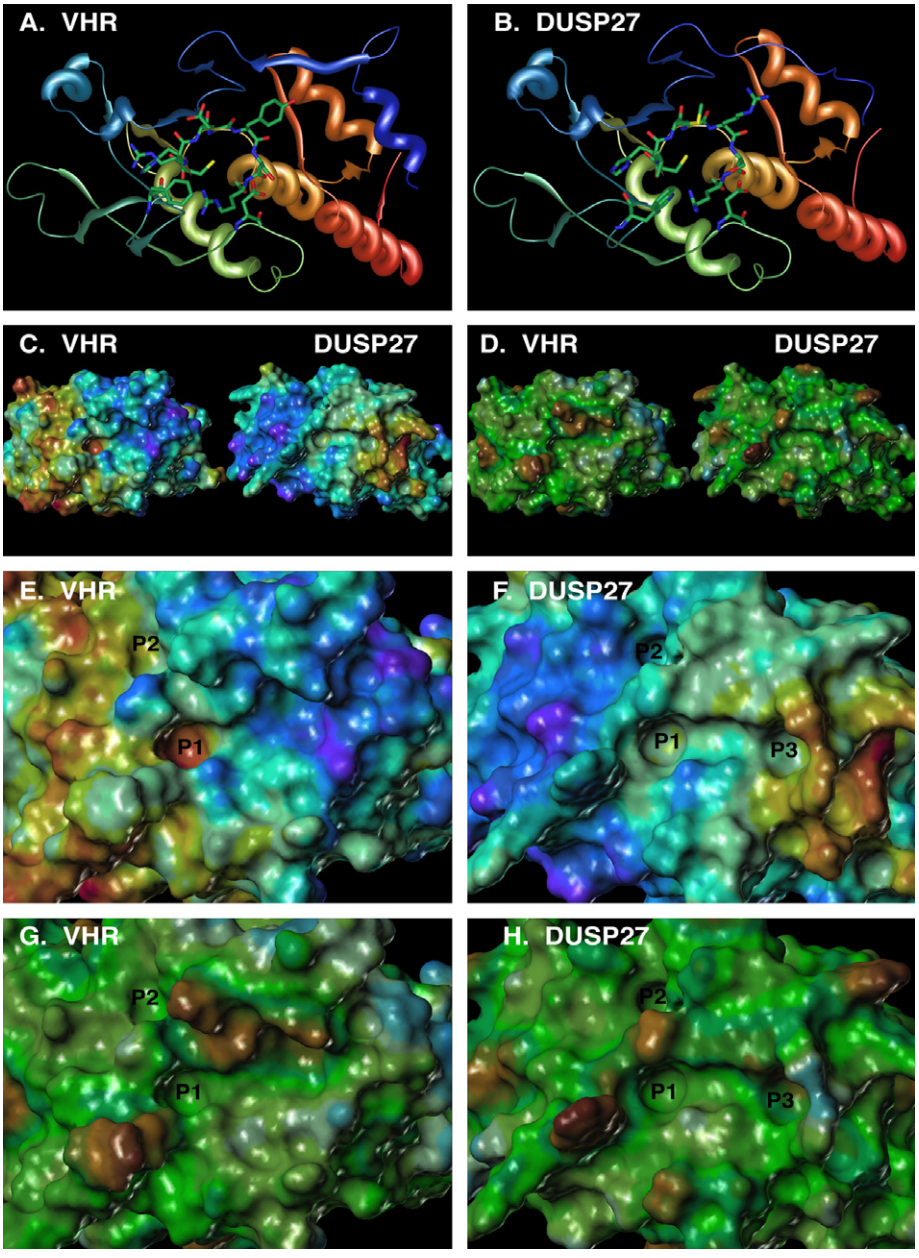

Fig. 3. Computer model of the three-dimensional structure of DUSP27. (A) and (B) Model of the α-helix/β-strand fold of DUSP27 compared to VHR (PDB code 1VHR). The cartoon was generated by using iMol version 0.30 (Pirx). (C) and (D), Comparison of substrate-binding surfaces of DUSP27 and VHR colored for electrostatic potential (C), and lipophilic potential (D). (E) and (F) Surface representation of active site of DUSP27 and VHR, colored for electrostatic potential. (G) and (H), Surface representation of active site of DUSP27 and VHR, colored for lipophilic potential. The molecular surfaces were generated with MOLCAD in SYBYL version 7.0 (Tripos), using the computer model of DUSP27 and the crystal structure of VHR. The color code of MOLCAD represents electrostatic potential (red, most positive; purple, most negative), and lipophilic potential (brown, more lipophilic; blue, more hydrophilic).

ported by additional findings: cDNA from human skeletal muscle was subjected to PCR, using primers corresponding to nucleotide sequences in the 5′ non-translated and in the 3′ non-coding regions. The obtained PCR product consisted of 821 bp, 41 of which are before the initiation codon, and 117 after the stop codon, the sequence of which is identical to the corresponding part of the gene in the NCBI gene bank. The presence of these regions indicates that the probability of additional upstream or down stream exons is very low. In addition, the size of mRNA from human skeletal muscle is about 1000 bp, as determined by Northern blotting (Fig. 1D). Finally, there is a stop codon 66 bp upstream the initiation codon. Taken together, these finding support the conclusion that the protein encoding part of the mRNA consists of 663 bp in three exons, which constitutes an ORF that translates into a 220-amino acid protein (Fig. 1E), with a perfect alignment with several known small DSPs, like VH1 related (VHR) (*DUSP3*), and the two products of the *DUSP13* gene(s), TMDP and BEDP. Thus, the new gene expresses a transcript with 3 exons that encode a regular member of the group of 'atypical' DSPs without any cyclophilin-like region. The original name *DUPD1* therefore is a misnomer and is now replaced by the designation *DUSP27* (Accession AAT94288).

3.2. DUSP27 is evolutionary conserved

Apparent species orthologs of DUSP27 (Fig. 2A) were found in a variety of organisms from primates (chimpanzee; 97% identity), other mammals (e.g., mouse, rat and dog, 87%, 86% and 81% identity, respectively), chicken (70% identity), to amphibians (*Xenopus tropicalis*; 76% identity) and fish (*Tetraodon*; 59% identity). The two proteins encoded by *DUSP13* (termed BEDP and TMDP) were also present in mammals and in chicken, and were 50–53% identical to DUSP27 in the same species, but such a combination of these enzymes was not detected in lower species. Thus, it appears

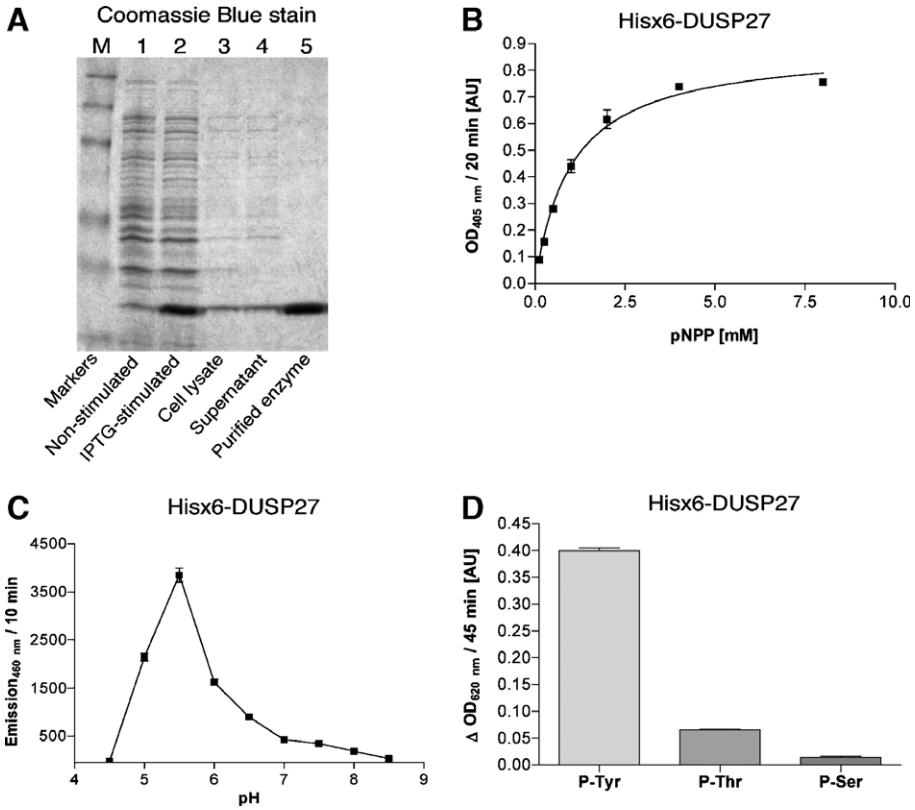

Fig. 4. Catalytic activity of recombinant DUSP27. (A) Coomassie Blue stain of SDS gel with samples from: Suspension of *E. coli* BL21(DE3) cells, transformed with pET28a(+) plasmid containing DUSP27 insert before induction (lane 1), or after IPTG induction (lane 2). Cell lysate (lane 3), and its supernatant, clarified by centrifugation (lane 4). The His_6-DUSP27 protein eluted from Ni-NTA-agarose beads (lane 5). (B) Michaelis–Menten kinetics His_6-DUSP27, using pNPP as a substrate. (C) pH profile of the His_6-DUSP27-catalyzed reaction. (D) Dephosphorylation of phosphotyrosine (P-Tyr), phosphothreonine (P-Thr), and phosphoserine (P-Ser), by His_6-DUSP27.

Table 1
Kinetics parameters of DUSP27 and related phosphatases

	DUSP27	VHZ[a]	VHI[a]	VHX[a]	VHY[a]
K_m (mM)	1.02 ± 0.091	1.498 ± 0.164	1.214 ± 0.067	0.412 ± 0.023	0.199 ± 0.014
K_{cat} (s^{-1})	0.30 ± 0.009	0.009 ± 0.0004	0.904 ± 0.016	0.400 ± 0.006	0.136 ± 0.002

[a]Refs. [10,11].

likely that a gene duplication event gave rise to the *DUSP27*/*DUSP13* pair prior to the divergence of mammals from the avian/dinosaur lineage more than 180 million years ago.

The canonical protein tyrosine phosphatase (PTP) (including DSPs) consensus sequence (HCX_2GX_2R) of DUSP27, HCVMGRSR, is unusual in that it has an arginine after the conserved glycine (Fig. 2B). This feature is also found in VHP [1], in the inactive tensin (*TNS*) and in PTPMT1 (MOSP in Ref. [1]). However, other InsP-specific phosphatases, including PTEN, tend to have a lysine residue at this location, as well as an additional lysine or arginine immediately after the catalytic cysteine, where DUSP27 has a valine. Thus, it is not likely that DUSP27 is an inositol-phosphate (InsP)-specific enzyme.

3.3. Three-dimensional model of DUSP27 structure

To further test the 3-exon ORF, we constructed a three-dimensional model of the DUSP27 protein. Using the 3-exon sequence, the protein was readily modeled on the template of

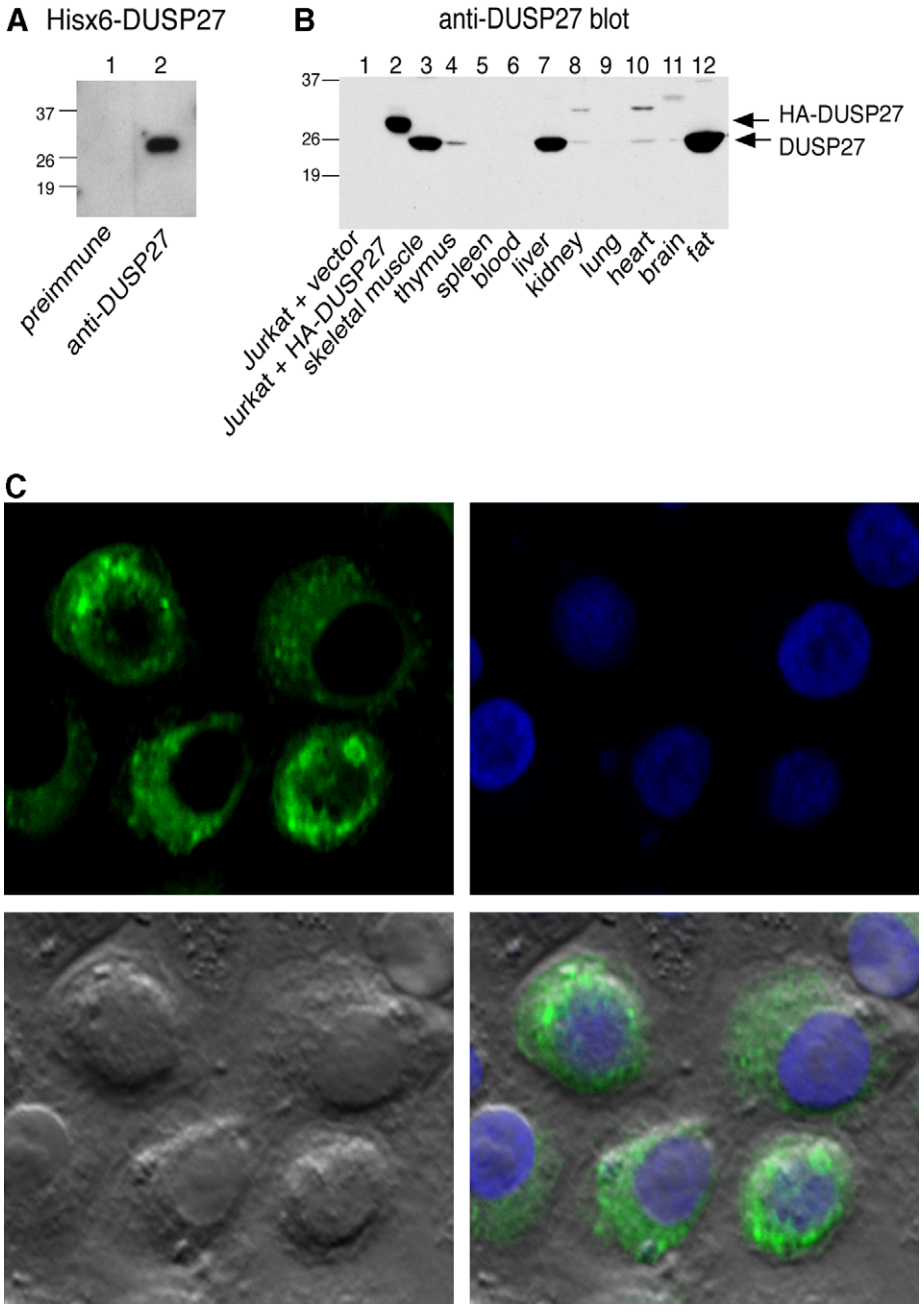

Fig. 5. Tissue expression and subcellular location of DUSP27. (A) Western blot of 10 ng recombinant DUSP27 resolved by SDS–PAGE using pre-immune serum (lane 1) or anti-DUSP27 antiserum (lane 2). (B) Western blot of Jurkat T cells transfected with empty vector (lane 1), with HA-DUSP27 (lane 2), or 100 μg of lysate from the indicated mouse tissues (lanes 3–12), with anti-DUSP27 antiserum. Note that the HA-DUSP27 is about 2 kDa larger then the endogenous DUSP27. This difference is probably due to the shorter mouse protein and to the addition of HA-tag. (C) Immunofluorescence staining of HeLa cells transfected with HA-DUSP27 using the Alexa Fluor® 488-conjugated anti-hemaggultinin (upper left panel). DNA was stained with DAPI (upper right panel) and a Nomarski phase contrast image also taken of the cells (lower left panel). A merge of the three images is shown in the bottom right panel. Note that DUSP27 staining is somewhat granular, and excluded from the nucleus.

crystallized DSPs, like VHR (Fig. 3A and B). Inserting the computationally predicted fourth exon between exons 2 and 3 results in the loss of the catalytic core machinery.

Interestingly, DUSP27 and VHR have reverse surface charge patterns on their substrate-facing aspect (Fig. 3C), i.e. DUSP27 is basic where VHR is acidic, and vice versa. The lipophilic potential, however, is similar in both enzymes (Fig. 3D). VHR was crystallized with a bound phosphopeptide corresponding to the activation loop of MAP kinases [9]. The phosphotyrosine residue of the phosphopeptide was anchored in the catalytic pocket ('P1' in Fig. 3E and G), while a second basic pocket ('P2') binds the phosphothreonine residue. The amino acid residue between these two phosphoresidues interacted with Q126 in VHR, which forms the ridge between the two pockets. In comparison, DUSP27 has more acidic surface (blue in Fig. 3C and F) surrounding the catalytic pockets (P1), while the second pocket (P2) is much more acidic, and it not likely to bind a phosphate. Furthermore, the ridge between the two pockets is formed by a methionine residue (M149), which would not interact with the peptide backbone of a substrate. Instead, in DUSP27, a trench leads to a putative basic pocket ('P3' in Fig. 3F and H). A dual-phosphorylated phosphopeptide would fit well into this grove, provided two amino acid residues would separate the phosphorylated residues, rather than one as in MAP kinase. Finally, the hydrophobicity patterns of VHR and DUSP27 are similar; both are largely hydrophilic and have two hydrophobic patches, one on each side of the catalytic pocket (Fig. 3G and H). In DUSP27, one of these is a tryptophan side chain that likely interacts with the incoming substrate, which therefore may be a phosphotyrosine, rather than a phosphoserine or phosphothreonine. Taken together, these models strongly suggest that the physiological substrates for DUSP27 are different than those of VHR.

3.4. DUSP27 is a catalytically active phosphatase

The DUSP27 DNA was inserted into a plasmid and introduced into *E. coli* to express recombinant DUSP27 protein (Fig. 4A). The expressed DUSP27 protein had catalytic activity, expressed by dephosphorylation of pNPP and DiFMUP (Fig. 4B and C). The kinetics parameters were found to be: K_m 1.02 ± 0.09 mM, V_{max} 0.132 ± 0.004 μM s^{-1} (determined with 0.4 μM DUSP27), K_{cat} 0.330 ± 0.009 s^{-1}, and K_{cat}/K_m 0.325 mM^{-1} s^{-1}. The pH optimum for DUSP27 was 5.5 (Fig. 4C). These kinetics parameters are similar to those obtained for other small DSPs (Table 1). Free phosphotyrosine was also a good substrate, while phosphothreonine and phosphoserine were much less readily dephosphorylated (Fig. 4D). Thus, it appears that DUSP27, like VHR [9], prefers phosphotyrosine. These findings are in agreement with the enzymatic specificity predicted by inspecting three-dimensional model of the enzyme (Section 3.3).

3.5. Tissue and cellular localization of DUSP27

Anti-DUSP27 antisera were obtained by immunizing rabbits with His_6-tagged full-length DUSP27 and they reacted very well with the recombinant protein (Fig. 5A), as well as with HA-tagged DUSP27 expressed in mammalian cells (Fig. 5B lane 2). The antiserum also reacted strongly with a protein of ~23 kDa in several mouse tissues, notably in skeletal muscle, liver, and fat (Fig. 5B). A weak band was seen in thymus, kidney and heart. Finally, confocal microscopy of HeLa cells transfected with hemagglutinin epitope-tagged DUSP27 (HA-DUSP27) and stained with the mAb against its epitope tag showed that DUSP27 is a cytosolic enzyme with a somewhat granular staining, but excluded from the nucleus (Fig. 5C).

In conclusion, we have begun the characterization of a novel DSP, which is highly expressed in skeletal muscle, adipose tissue and liver, central tissues for energy metabolism. Future experiments will elucidate whether DUSP27 is involved in the regulation of energy metabolism.

Note added in proof

Recent alterations in the phosphatase nomenclature by HUGO-Gene Nomenclature Committee establish the name DUSP27 for the enzyme described in this paper (aliases: DUPD1; FMDSP), whereas the putative enzyme formerly called DUSP27 is now designated STYXL2.

Acknowledgement: This work was supported by National Institutes of Health Grant AI35603.

References

[1] Alonso, A. et al. (2004) Protein tyrosine phosphatases in the human genome. Cell 117, 699–711.
[2] Pagliarini, D.J. et al. (2005) Involvement of a mitochondrial phosphatase in the regulation of ATP production and insulin secretion in pancreatic cells. Mol. Cell. 19, 197–207.
[3] Lv, B.F. et al. (2006) Protein tyrosine phosphatase interacting protein 51 (PTPIP51) is a novel mitochondria protein with an N-terminal mitochondrial targeting sequence and induces apoptosis. Apoptosis 11, 1489–1501.
[4] Huynh, H. et al. (2004) Control of vesicle fusion by a tyrosine phosphatase. Nat. Cell Biol. 6, 831–839.
[5] Srivastava, S. et al. (2005) The phosphatidylinositol 3-phosphate phosphatase myotubularin-related protein 6 (MTMR6) is a negative regulator of the Ca^{2+}-activated K^+ channel KCa3.1. Mol. Cell Biol. 25, 3630–3638.
[6] Merkulova, M. et al. (2005) Secretion of the mammalian Secl4p-like phosphoinositide-binding p45 protein. FEBS J. 272, 5595–5605.
[7] Bujnicki, J.M., Elofsson, A., Fischer, D. and Rychlewski, L. (2001) Structure prediction meta server. Bioinformatics 17, 750–751.
[8] Schwede, T., Kopp, J., Guex, N. and Peitsch, M.C. (2003) SWISS-MODEL: an automated protein homology-modeling server. Nucleic Acids Res. 31, 3381–3385.
[9] Schumacher, M.A. et al. (2002) Structural basis for the recognition of a bisphosphorylated MAP kinase peptide by human VHR protein phosphatase. Biochemistry 41, 3009–3017.
[10] Alonso, A. et al. (2004) VHY, a novel myristoylated testis-restricted dual specificity protein phosphatase related to VHX. J. Biol. Chem. 279, 32586–32591.
[11] Alonso, A. et al. (2004) The minimal essential core of a cysteine-based protein-tyrosine phosphatase revealed by a novel 16-kDa VH1-like phosphatase, VHZ. J. Biol. Chem. 279, 35768–35774.